Chapter 7
Precipitation Hardening

Abstract Models for precipitation hardening (PH) at room temperature have been available for a long time. In spite of the importance of PH, it took a long time to establish models for elevated temperatures. In fact, empirically the room temperature models have also been used at higher temperatures. This gives the wrong temperature dependence and overestimates PH. It was for a long time thought that it was an energy barrier for climb across particles that was the controlling mechanism, but it was gradually appearing that this effect was so small that it could be neglected. Instead it is time it takes for dislocations to climb across particles that is the critical factor. Small particles are readily passed and do not contribute to the strengthening. Particles larger than a critical size have to be passed by the Orowan mechanism, because there is not time enough for dislocations to climb across these particles. This mechanism was finally verified for Cu–Co alloys.

7.1 General

The precipitation of phases in the form of particles is probably the most effective way of increasing the creep strength in alloys. Precipitation hardening is utilized in many types of steels and Ni-base alloys. Because of its technical significance there are a large number of publications on precipitation hardening in these alloy systems. The role of carbides and nitrides in Cr–Mo steels and γ' in Ni-base alloys has been extensively studied. It is well established that the presence of fine precipitates in these systems is essential to get good creep strength.

The understanding of precipitation hardening (PH) at ambient temperatures has been well established for a long time. However, in spite of its technical importance, this has not been the case for the role of precipitation hardening during creep. Only recently, a satisfactory description has been formulated. In fact, many scientists have tried to use models developed for applications at ambient temperatures for PH at elevated temperatures. This does not work well because methods at ambient temperatures are essentially temperature independent. The temperature dependence they involve is often only that of the shear modulus and that is weak. However, the

R. Sandström, *Basic Modeling and Theory of Creep of Metallic Materials*, Springer Series in Materials Science 339,
https://doi.org/10.1007/978-3-031-49507-6_7

creep rate and strength typically decrease exponentially with increasing temperature (see Chap. 2) and this is strongly at variance with models for applications at ambient temperatures.

It was early on recognized that climb must play an important role for describing PH. It was thought that there is a significant energy barrier for dislocations to climb across particles. More and more accurate models for the energy barrier were developed. However, at the same time the predicted size of the energy barrier decreased when new models were presented. Eventually the magnitude became so small that they were no longer near to explain the large size of PH observed in commercial alloys. This development will briefly be summarized in Sect. 7.2.

It was evident that an entirely new principle was needed to understand PH. The solution was to assume that it is the time for a dislocation to climb across a particle rather than the size of the energy barrier that is the controlling factor [1]. A critical particle size is introduced. If a particle is large enough, there will not be sufficient time to get across it and the particle will block the motion of the dislocation. This gives a contribution to the creep strength. On the other hand if the particles are small they will readily be climbed across and they will not contribute to the creep strength. With this model is has been possible to describe PH of 9 and 12Cr steels, austenitic stainless steels and Cu–Co alloys [2–4]. The model development will be presented in Sect. 7.3. The application to Cu–Co alloys is covered in Sect. 7.4.

7.2 Previous Models for the Influence of Particles on the Creep Strength

7.2.1 Threshold Stress

At about half the absolute melting point T_m, many particle free materials have a stress exponent n_N for the creep rate in the interval 4–7. Particle strengthened alloys typically have a higher stress exponent. This can be rationalized if the creep rate $\dot{\varepsilon}$ is expressed as

$$\dot{\varepsilon} = A_n(\sigma - \sigma_i)^{n_i} \tag{7.1}$$

σ is the applied stress, σ_i the internal stress from the particles, and A_n and n_i constants. With this formulation, the stress exponent n_i is smaller than n_N. As can be seen from the analysis in Chap. 2, an equation of the type in Eq. (7.1) can be derived from basic principles so the equation has a good basis. In a number of papers, σ_i, A_n and n_i have been used as adjustable parameters to make Eq. (7.1) fit the experiments and to have n_i to fall in the range 4–7. A special procedure called the Lagneborg-Bergman plot was developed for this purpose [5].

Assuming that σ_i is constant which was frequently done, it implies that σ_i is a threshold stress and below this stress no creep will take place. For oxide dispersion

strengthened alloys (ODS) such a threshold stress has been observed [6, 7], but there are also ODS where a threshold is not found. However, for most particle strengthened materials for example the common CrMo steels, no threshold stress has been recorded. By analyzing Eq. (7.1), it is found that the stress exponent n_N decreases with increasing stress. This behavior is observed for a few ODS alloys [7], but not for most particle strengthened alloys, which is a drawback of the model.

The reasons for the failure of the assumption with a constant threshold stress are now well understood. It is now possible to derive σ_i directly. In fact, it is shown later in this chapter that σ_i is not a constant. It depends on both temperature and stress and there is no indication that it will tend to a limiting value at low stresses.

7.2.2 Orowan Model

Dislocations can pass particles by cutting through them, by flowing around them or climbing across them. At ambient temperatures only the first two are usually considered. Particle cutting will not be analyzed in the present text because as we will see later in this chapter, it is unlikely that it is of importance in creep exposed materials except in special cases. For a summary of mechanisms for particle cutting, see [8].

The Orowan model for dislocation looping of particles will briefly be described here because it is needed in Sect. 7.3. When the stress increases for a dislocation attached to particles, the dislocation will eventually almost meet itself around the particles. The maximum force F that the dislocation can take is $2\tau_L \approx 2Gb^2/2$ where τ_L is the dislocation line tension. The external force F on a dislocation segment of length λ is (Peach-Koehler formula)

$$F = \sigma\lambda b/m_T \tag{7.2}$$

where σ is the external stress and m_T is the Taylor factor. By equating the two forces the critical stress is obtained. This is the stress for Orowan looping σ_O

$$\sigma_O = \frac{m_T C_O G b}{\lambda} \tag{7.3}$$

Many refinements of this expression are available in the literature. However, they can approximately be taken into account by adding a factor $C_O = 0.8$ [9]. The precision in the prediction of PH does not justify that a more elaborate formulation is needed. λ is usually assumed to be taken as the nearest neighbor distance for randomly distributed spherical particles of radius r and a volume fraction of f_V. This distance is usually referred to as the planar lattice square spacing λ_s

$$\lambda_s = r(2\pi/3f_V)^{1/2} \tag{7.4}$$

As can be seen from Eqs. (7.3) and (7.4), the Orowan strength increases with decreasing particle radius and increasing volume fraction of particles.

As pointed out above, the Orowan strength has been used many times to estimate the influence of particles on the creep strength. This overestimates the strength contribution since Eq. (7.3) is only weakly temperature dependent through the shear modulus G, which decreases approximately linearly with temperature.

7.2.3 The Role of the Energy Barrier

Many attempts were made in the past to generalize the Orowan model by taking climb into account. For a review, see [7, 10]. Initial attempts to determine the size of the energy barrier and the associated value for σ_i were made by Brown and Ham [9] and by Lagneborg [11]. They found a value for internal stress σ_i of about half the Orowan stress, which was in agreement with observations for some materials. However, they assumed the presence of local dislocations that were attached to the particles and that the dislocations remained in the glide planes between the particles. This introduces sharp bends on the dislocations that are easily relaxed. Further modeling therefore concentrated to general dislocations that are only attached to a single point on the particles and have more general degrees of freedom. The assumption about climb of general dislocations rather than of local dislocations is clearly more realistic. However, with this approach the values for σ_i turned out to be quite small and tended to decrease with each investigation [6, 7, 12]. The best estimate for the minimum climb stress σ_{clmin} is [6, 7]

$$\frac{\sigma_{clmin}}{\sigma_O} = \frac{\alpha_{cl}}{\alpha_{cl} + 2C_O} \tag{7.5}$$

where

$$\alpha_{cl} = \frac{2\bar{r}}{3\lambda_s} = \sqrt{\frac{2f_V}{3\pi}} \tag{7.6}$$

α_{cl} is called the climb resistance. This gives a value of 0.02–0.06 for σ_{clmin} of the Orowan stress for common particle volume fractions of $f_V = 1$ to 5%.

The predicted energy barriers are so low that they are of little practical value to describe the significant PH in engineering alloys. One possibility is that there is an attractive interaction between the dislocations and the particles. Such an interaction has been observed for ODS [13, 14] but not in general for other PH systems. This behavior has also been modeled [15, 16]. The dilemma with this model is that the interaction strength is considered as an adjustable parameter and this means that the model is not predictive. The nature of the interaction cannot therefore be ascertained.

Clearly, the energy barriers against climb cannot be used as a basis for explaining PH. Instead another approach will be presented in Sect. 7.3 that is based on the time it takes for a dislocation to climb across a particle.

7.3 Precipitation Hardening Based on Time Control

It is evident from the summary in Sect. 7.2.3 that an energy barrier against climb cannot be the controlling factor for the role of precipitates during creep. For this reason, an alternative approach is considered. The following assumptions are involved [1, 2, 4]

- Precipitation hardening is considered but not oxide dispersion strengthening (ODS). This means that the attractive interaction that sometimes appears for ODS alloys is not taken into account.
- The controlling mechanism is assumed to be the time it takes for a dislocation to climb across a particle, not an energy barrier. It is this time that decides whether a particle will be climbed or not.
- The critical particles radius r_{crit} is taken for the largest particle where there is sufficient time for the dislocation to climb across.
- For particles smaller than r_{crit} they will freely be climbed across and will not contribute to the creep strength.
- Particle shearing is not taken into account since small particles will be passed by climb anyway.
- Particles larger than r_{crit} have to be passed by Orowan bowing and this determines their contribution to the creep strength.

These principles for PH have for example been used for austenitic stainless steel [3, 17–19]. The total creep strength has been possible to predict in a precise way.

For climb to be of importance, the climb time t_{climb} must be as long as the glide time t_{glide} between particles. This criterion can be used to find the critical particle radius

$$t_{\text{climb}} = t_{\text{glide}} \tag{7.7}$$

The critical radius r_{crit} is equal to the climb time multiplied by the climb velocity v_{climb}

$$t_{\text{climb}} = \frac{r_{\text{crit}}}{v_{\text{climb}}} \tag{7.8}$$

The climb velocity can be derived from the climb mobility, Eq. (2.29)

$$v_{\text{climb}} = M_{\text{climb}}(T, \sigma) b \sigma \tag{7.9}$$

where σ is the applied stress. The glide time t_{glide} is controlled by the average distance between particles λ_s

$$t_{\text{glide}} = \frac{\lambda_s}{v_{\text{glide}}} \tag{7.10}$$

The Orowan equation for the creep rate gives the glide velocity

$$\dot{\varepsilon} = v_{\text{glide}} \frac{b\rho}{m_T} \tag{7.11}$$

where ρ is the dislocation density. From Eqs. (7.7) to (7.11) an expression for the critical radius can be derived.

$$r_{\text{crit}} = M_{\text{climb}}(T, \sigma) b^2 \sigma \lambda_F \frac{\rho}{\dot{\varepsilon}_{\text{sec}} m_T} \tag{7.12}$$

The secondary creep rate $\dot{\varepsilon}_{\text{sec}}$ is given by Eq. (2.30). In Eq. (7.12) the Friedel spacing between the particles λ_F has been introduced. It is thought that it is the best way of representing the average distance between the pinning points along the dislocations and it is a better alternative than the planar lattice square spacing λ_s [7, 8]. λ_F can be related to the force acting on a climbing segment

$$\left(\frac{\lambda_s}{\lambda_F}\right)^2 = \frac{F}{2\tau_L} = \frac{\sigma_{\text{clmin}} b \lambda_F}{2 m_T \tau_L} = \frac{\sigma_{\text{clmin}}}{\sigma_O} \frac{\lambda_F}{\lambda_s} \tag{7.13}$$

In deriving Eq. (7.13), Eqs. (7.2) and (7.3) have been used. By applying also Eq. (7.5), we find that

$$\left(\frac{\lambda_s}{\lambda_F}\right)^3 = \frac{\alpha_{cl}}{\alpha_{cl} + 2C_O} \tag{7.14}$$

With the help of Eqs. (7.4), (7.6) and (7.14), the Friedel spacing can be derived.

To determine the contribution from the particles to the strength, their size distribution must be known. Particles of significance in creep resistant materials often follow an exponential size distribution [2, 18]. Then the number of particles per unit area N_A can be expressed as

$$N_A = N_{A0} e^{-k(r - r_0)} \tag{7.15}$$

where $N_{A0} = 1/\lambda_s^2$, and r is the particle radius. r_0 takes into account that there are often no accurate observations at small particle sizes; r_0 is taken as 1 μm for scanning microscopy. k is related to the average particle size $\bar{r}$ as $k = 1/(\bar{r} - r_0)$. As pointed out above only particles larger than r_{crit} contribute to the creep strength. Thus the average spacing between these particles λ_{crit} is an important quantity

$$\lambda_{\text{crit}} = \sqrt{N_{A0}} e^{-k(r_{\text{crit}} - r_0)/2} \tag{7.16}$$

The contribution to the creep strength can then be expressed as

$$\sigma_{\text{part}} = \frac{C_{\text{O}} G b m_{\text{T}}}{\lambda_{\text{crit}}} = \sigma_{\text{O}} e^{-k(r_{\text{crit}} - r_0)/2} \tag{7.17}$$

This contribution is added to σ_{i} in Eq. (2.30). The critical radius depends on temperature and stress and consequently, so does σ_{part}.

7.4 Application of the Precipitation Hardening Model

7.4.1 Analyzed Materials

The model in Sect. 7.3 was first published in 2000 and was successfully applied both to Cr–Mo steels [2] and to austenitic stainless steels [1, 3, 17]. In these applications, PH is not the dominating contribution to the creep strength. Therefore they could not be considered as full verification of the PH model. In this section results on creep in Cu–Co alloys published by Wilshire and coworkers will be analyzed [20, 21]. This system has the advantage that the particles have a large influence on the creep rate. In addition, several ageing conditions with different particle size distributions were studied, so the influence of the particles can safely be ascertained. A valuable feature is that the effect of solid solution hardening in these studies is negligible small as will be shown and will not interfere with the analysis.

The analyzed alloys and conditions are summarized in Table 7.1.

Three alloys were included in the study with 0.88, 2.48 and 4.04 wt.% Co. In their main condition the alloys were fully aged at 600 and 700 °C generating a stable particle structure. These temperatures were sufficiently high that no particle

Table 7.1 Investigated Cu–Co alloys

Co, wt.%	Heat treatment temperature, °C	Heat treatment type	Particle volume fraction	Co in solid solution, wt.%	Particle radius, nm	Particle spacing, nm	Orowan stress, MPa
0.88	600	Underaged	0.00567	0.33	1.2	41	593
0.88	600	Aged	0.00567	0.33	4.2	98	250
0.88	600	Overaged	0.00567	0.33	17.2	405	60
2.48	600	Aged	0.0222	0.33	7.6	90	272
4.04	700*	Aged	0.0344	0.33*	22.6	215	113

* Stabilized at 600 °C after heat treatment at 700 °C

Reprinted from [4] with permission of Springer

coarsening took place during the creep testing at 439 °C. In addition, underaged and overaged conditions were covered for the 0.88 wt.% alloy.

The volume fraction of particles for the different alloys and the amount of Co were calculated with the thermodynamic software Thermo-Calc, see Table 7.1. The particle sizes were measured with transmission electron microscopy [20, 21]. Using the expression for the square lattice spacing, Eq. (7.4), the particle spacing was determined. With the help of Eq. (7.3) the Orowan strength for the alloys was computed, see Table 7.1. The Orowan strength significantly exceeds the creep strength of the alloys as will be seen.

The amount of solid solution hardening of the alloys was evaluated with the help of Eq. (6.22). Some of the Co is in solid solution, Table 7.1. The computed solute drag stress was in the interval from 0.15 to 0.25 MPa, which is negligible in the context.

7.4.2 Pure Copper

To demonstrate the validity of PH model, it is essential to verify that strength contribution from the dislocations can be described with the model in Chap. 2. This is tested for pure copper. Some creep data for pure copper can be found in [20, 21]. In addition creep data have been taken from [22] where tests were performed at 400–500 °C that are close to the test temperature for the Cu–Co alloys. The creep rate versus applied stress is shown in Fig. 7.1.

From Fig. 7.1 it can be seen that the predicted temperature dependence is larger than the observed one. The reason is that the activation energy for creep is lower than the activation energy of self-diffusion which is used in the prediction. That the

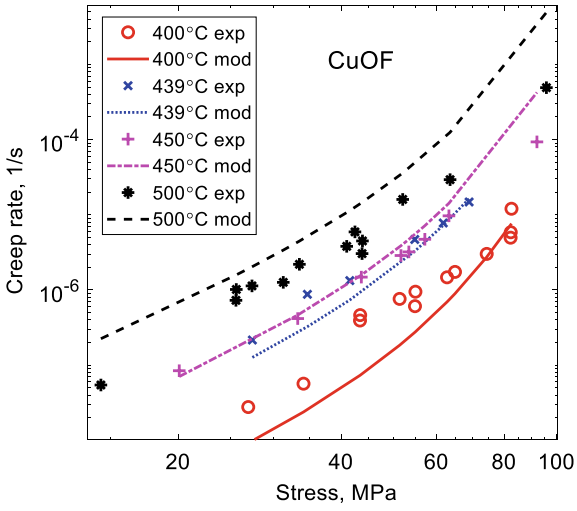

Fig. 7.1 Modeling of stationary creep rate (Eq. (2.29)) for Cu-OF at different test temperatures compared with experimental data [20–22]. Redrawn from [4] with permission of Springer

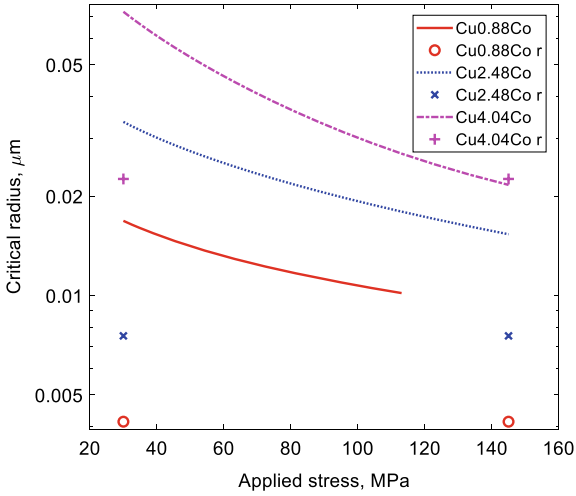

Fig. 7.2 Critical radius, Eq. (7.12) versus applied stress for three Cu–Co alloys. The average particle radiir are included for comparison, Table 7.1

activation energy for creep is lower than that for self-diffusion is unusual. This has been discussed by Raj and Langdon [22]. The stress exponent, i.e. the slope of the curves in Fig. 7.1 is in acceptable agreement with the observations. The model and experimental values at 439 and 450 °C are in close agreement.

7.4.3 Cu–Co Alloys

Only particles larger than the critical size contribute to the creep strength. Such particles have to be passed by Orowan bowing. The critical particles radius is given by Eq. (7.12). The critical particle radii for the three Cu–Co alloys is illustrated in Fig. 7.2.

In Fig. 7.2 in addition to the critical radii, the average particle sizes are shown. Both the typical radii and the critical radii increase with the Co content. At low stresses the critical radii are about a factor of four larger than the average particle radii. At larger stresses the difference is smaller. For the two lower Co contents it is a factor of two. For the highest Co content, there is no longer any difference anymore. This means that all particles contribute to the creep strength.

When the volume fraction and the average radius are known, the size distribution can be estimated with the help of Eq. (7.15). The result is illustrated in Fig. 7.3.

Exponential size distributions imply that the number of particles per unit area can decrease quite rapidly with increasing radius. The Co content has a large impact on the slope of the size distributions. The critical radii are marked in Fig. 7.3 for different applied stresses. As is evident from Fig. 7.2, the largest critical radii correspond to the lowest stresses.

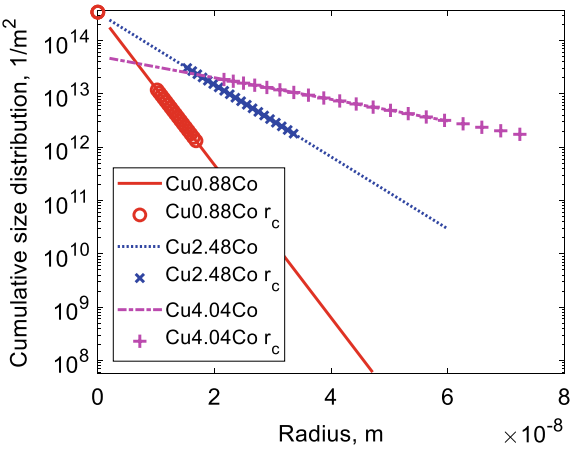

Fig. 7.3 Particle size distributions, Eq. (7.15) for the three Cu–Co alloys in aged condition with critical radii marked, Eq. (7.12)

The influence of particles on the creep strength is via the critical Orowan strength in Eq. (7.17). This strength is added to internal stress in Eq. (2.29). The critical Orowan strength is shown in Fig. 7.4.

The critical strength increases with the applied stress. It might be thought that if the Co content is raised it would automatically enhance PH. From Fig. 7.4 it is clear that this is not the case. In fact, the alloy with 2.48 wt.% Co gives the highest strength. The predicted creep rate as a function of applied stress is shown in Fig. 7.5.

The Co particles reduce the creep rate by about two orders of magnitude in relation to that of pure copper. It is evident that the model can reproduce this behavior quite well. The ranking of the three Cu–Co alloys is also in accordance with experiments. The stress dependence is handled in an acceptable way.

If Figs. 7.4 and 7.5 are compared, the difference in critical Orowan stress is directly related to the observed relations between the creep rates as proposed by the model.

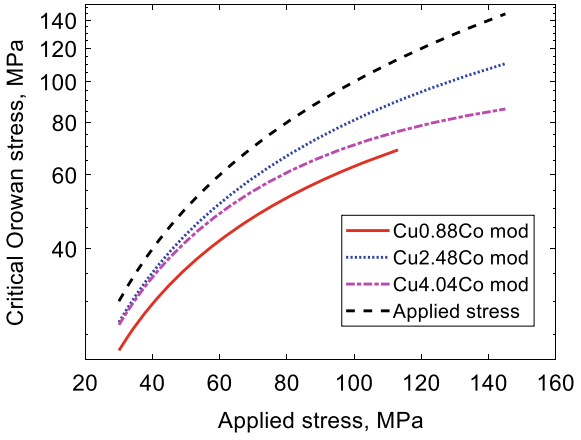

Fig. 7.4 Critical Orowan stress, Eq. (7.17) versus applied stress for three Cu–Co alloys. For comparison, a 1:1 line for the applied stress is included in the diagram. Redrawn from [4] with permission of Springer

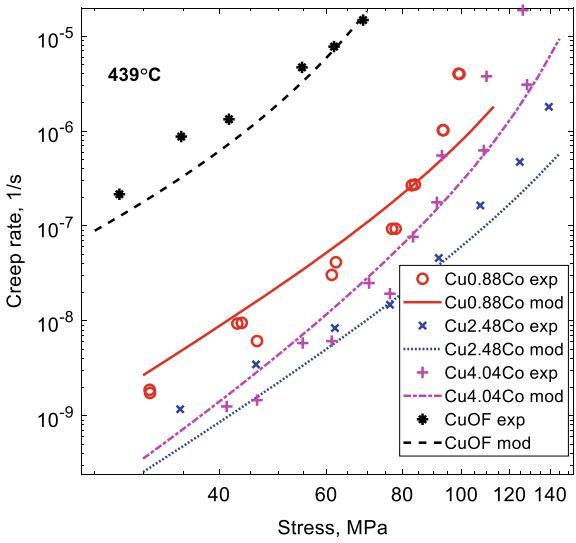

Fig. 7.5 Modeling of stationary creep rate for three Cu–Co alloys and pure copper compared with experimental data from [20]. Redrawn from [4] with permission of Springer

If the values for the Orowan strength at room temperature (Table 7.1) would be used to rank the creep strength it would suggest that Cu0.88Co and Cu2.48Co would have about the same creep strength and would be significantly better than Cu4.04Co. This is clearly not consistent with the model or with the experimental results. Another way of demonstrating that creep strength is not close related to the Orowan strength is illustrated in Fig. 7.6.

It can be seen that the ratio between the critical Orowan strength and room temperature Orowan strength varies with applied stress and alloy composition.

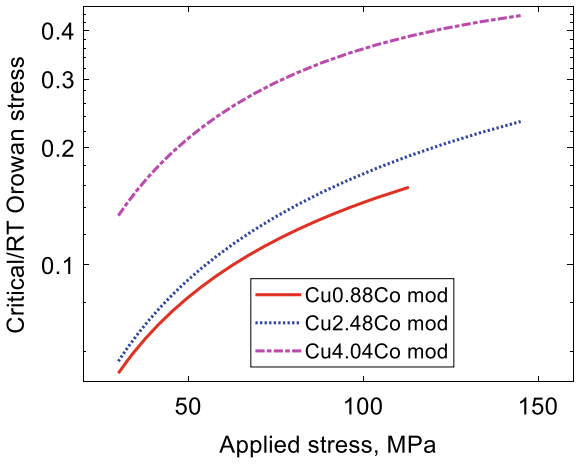

Fig. 7.6 Critical Orowan stress, Eq. (7.17), divided by the room temperature Orowan stress, Eq. (7.3) versus applied stress for three Cu–Co alloys. Redrawn from [4] with permission of Springer

In [20] there is also a comparison between underaged, aged and overaged conditions for the Cu0.88Co alloy. The computed size distributions for these conditions are shown in Fig. 7.7.

There is obviously a large difference between these conditions which makes it an interesting additional test of the model. Furthermore the size distributions are different from those in Fig. 7.3. The strain rate versus stress curves are presented in Fig. 7.8.

As can be seen in the Figure, the model can describe the experimental data fairly well. The difference between the conditions can be accounted for, and the stress dependence is well reproduced.

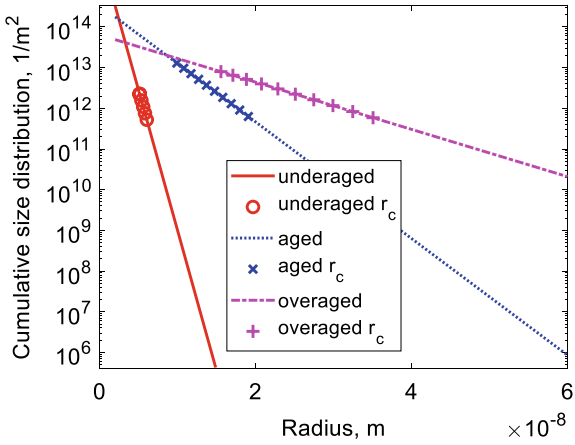

Fig. 7.7 Size distributions, Eq. (7.15) for Cu0.88Co particles in aged, underaged and overaged conditions with critical radii marked, Eq. (7.12). Redrawn from [4] with permission of Springer

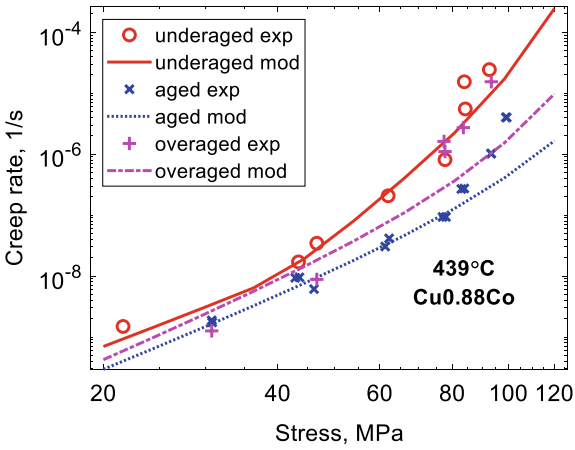

Fig. 7.8 Modeling of stationary creep rate, Eq. (2.29) with the internal stress taken from Eq. (7.17) for Cu0.88Co in underaged, aged and overaged conditions compared with experimental data from [20]. Redrawn from [4] with permission of Springer

7.5 Summary

- Empirical models for the influence of particles on the creep strength have often simply used the Orowan model. This has the consequence that the strong temperature dependence is almost completely neglected and hardening effect is exaggerated.
- Traditional systematic models for precipitation hardening during creep have been based on energy barriers. However, assessment of the size of the energy barriers has shown that it is negligibly small. Instead the modeling in this chapter is starting from the assumption that the time it takes for a particle to be climbed is the factor that controls if the particle contributes to the creep strength or not.
- A critical particle size is introduced. Particles that are smaller than the critical size do not contribute to the creep strength. Particles larger than the critical size must pass particles by Orowan bowing and they contribute to the creep strength.
- To find the critical particle size, the particle size distribution must be known. Exponential size distributions have been assumed. Such distributions have been found a number of times for creep resistant steels.
- A critical test has been performed for Cu–Co alloys. This is a suitable system since the amount of solid solution hardening is quite small. The model can account for the reduction in creep rate due to the presence of Co particles in Cu.
- Observed effects of Co content, heat treatment condition and stress dependence on the creep rate can be satisfactorily reproduced.
- The predicted increase in the creep strength is significantly smaller than the Orowan strength (except at high stress and high alloy content). The ratio between the predicted increase in strength and the Orowan strength varies with applied stress, Co-content and ageing condition.

References

1. J. Eliasson, A. Gustafson, R. Sandstrom, Kinetic modelling of the influence of particles on creep strength. Key Eng. Mater. **171–1**, 277–284 (2000)
2. H. Magnusson, R. Sandstrom, The role of dislocation climb across particles at creep conditions in 9–12 pct Cr steels. Metall. Mater. Trans. A **38A**, 2428–2434 (2007)
3. S. Vujic, R. Sandstrom, C. Sommitsch, Precipitation evolution and creep strength modelling of 25Cr20NiNbN austenitic steel. Mater. High Temp. **32**, 607–618 (2015)
4. F. Sui, R. Sandström, Creep strength contribution due to precipitation hardening in copper–cobalt alloys. J. Mater. Sci. **54**, 1819–1830 (2019)
5. R. Lagneborg, B. Bergman, The stress/creep rate behaviour of precipitation-hardened alloys. Metal Sci. **10**, 20–28 (1976)
6. E. Arzt, M.F. Ashby, Threshold stresses in materials containing dispersed particles. Scr. Metall. **16**, 1285–1290 (1982)
7. W. Blum, B. Reppich, Creep of particle-strengthend alloys, in *Creep Behaviour of Crystalline Solids*. ed. by B. Wilshire, R.W. Evans (Pineridge Press, Swansea U.K., 1985), p.83
8. J.W. Martin, *Precipitation Hardening*, 2nd edn. (Butterworth-Heinemann, Oxford, England, Woburn, Massachusetts, 1998)

9. L.M. Brown, R.K. Ham, *Strengthening Methods in Crystals*, in, Appl. Sci. Publ.. Ltd., (1971), p. 9
10. M. Heilmaier, B. Reppich, Particle threshold stresses in high temperatures yielding and creep: a critical review, in *Creep Behavior of Advanced Materials for the 21st Century, The Minerals, Metals and Materials Society* (1998), pp. 267–281
11. R. Lagneborg, Bypassing of dislocations past particles by a climb mechanism. Scr. Metall. **7**, 605–613 (1973)
12. R.S.W. Shewfelt, L.M. Brown, High-temperature strength of dispersion-hardened single crystals II. Theory Philos. Mag. **35**, 945–962 (1977)
13. V.C. Nardone, J.K. Tien, Pinning of dislocations on the departure side of strengthening dispersoids. Scr. Metall. **17**, 467–470 (1983)
14. J.H. Schröder, E. Arzt, Weak beam studies of dislocation/dispersoid interaction in an ods superalloy. Scr. Metall. **19**, 1129–1134 (1985)
15. E. Arzt, J. Rösler, The kinetics of dislocation climb over hard particles—II. Effects of an attractive particle-dislocation interaction. Acta Metall. **36**, 1053–1060 (1988)
16. J. Rösler, E. Arzt, The kinetics of dislocation climb over hard particles—I. Climb without attractive particle-dislocation interaction. Acta Metall. **36**, 1043–1051 (1988)
17. R. Sandström, Fundamental models for creep properties of steels and copper. Trans. Indian Inst. Met. **69**, 197–202 (2016)
18. R. Sandström, M. Farooq, J. Zurek, Basic creep models for 25Cr20NiNbN austenitic stainless steels. Mater. Res. Innov. **17**, 355–359 (2013)
19. J. He, R. Sandström, Basic modelling of creep rupture in austenitic stainless steels. Theoret. Appl. Fract. Mech. **89**, 139–146 (2017)
20. P.L. Threadgill, B. Wilshire, Effect of particle size and spacing on creep of two-phase copper—Cobalt alloys. Metal Sci. **8**, 117–124 (1974)
21. J.D. Parker, B. Wilshire, The effect of a dispersion of cobalt particles on high-temperature creep of copper. Metal Sci. **9**, 248–252 (1975)
22. S.V. Raj, T.G. Langdon, Creep behavior of copper at intermediate temperatures-I. Mechanical characteristics, Acta Metall. **37**, 843–852 (1989)